Food & Function

Accepted Manuscript

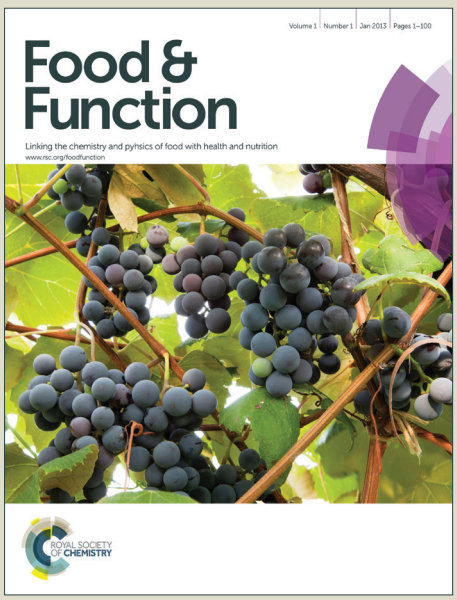

This is an *Accepted Manuscript*, which has been through the Royal Society of Chemistry peer review process and has been accepted for publication.

Accepted Manuscripts are published online shortly after acceptance, before technical editing, formatting and proof reading. Using this free service, authors can make their results available to the community, in citable form, before we publish the edited article. We will replace this *Accepted Manuscript* with the edited and formatted *Advance Article* as soon as it is available.

You can find more information about *Accepted Manuscripts* in the Information for Authors.

Please note that technical editing may introduce minor changes to the text and/or graphics, which may alter content. The journal's standard Terms & Conditions and the Ethical guidelines still apply. In no event shall the Royal Society of Chemistry be held responsible for any errors or omissions in this *Accepted Manuscript* or any consequences arising from the use of any information it contains.

ROYAL SOCIETY OF CHEMISTRY

www.rsc.org/foodfunction

Polysaccharide from *Pleurotus nebrodensis* induces apoptosis via mitochondrial pathway in HepG2 cells

Haiyan Cui, Shufen Wu, Yanping Sun, Tiantian Wang, Zhenjing Li, Mianhua Chen, Changlu Wang*

* Corresponding author (Changlu Wang).

Address:

Key Laboratory of Food Nutrition and Safety, Ministry of Education, School of Food Engineering and Biotechnology, Tianjin University of Science and Technology, Tianjin 300457, PR China

Tel: +86 22-6027-2219

Fax: +86 22-6027-2219

E-mail address: clw123@tust.edu.cn

Abstract

A novel alkali extractable polysaccharide (designated as PNA-2) was purified from *Pleurotus nebrodensis* and the effects of purified PNA-2 on the proliferation and apoptosis of human hepatic cancer cells (HepG2) were investigated in this study. The results of 3-(4,5-dimethylthiazol-2-yl)-2,5-diphenyltetrazolium bromide (MTT) assay indicated that PNA-2 inhibited the proliferation of HepG2 cells by apoptosis induction, which was also characterized by scanning electron micrographs (SEM). Moreover, expressions of apoptosis-associated mRNA, proteins and cell-cycle arrest of G0/G1 phase were determined by RT-qPCR, western blot and flow cytometry, respectively. A notable inhibition of the migration rate of PNA-2-treated HepG2 cells was observed by the cell scratch assay. DNA damage was observed by the comet assay and AO/EB staining in HepG2 cells, which were exposed to PNA-2. Induction of mitochondria-mediated intrinsic apoptotic pathway by PNA-2 was evidenced by the loss of mitochondrial membrane potential ($\Delta\Psi m$), bcl-2 dysregulation and cytochrome c release. All results suggested that mitochondria-mediated intrinsic apoptotic pathway could be involved in PNA-2 -mediated apoptosis of human liver carcinoma cell HepG2. Finally, the results indicated that PNA-2 significantly suppressed tumor growth through the mitochondrial pathway in HepG2 tumor-bearing mice, which , indicating that PNA-2 may be developed as a candidate drug or function food factor to prevent or treat liver cancer.

Keywords: *Pleurotus nebrodensis*; polysaccharide; apoptosis; mitochondrial pathway

1. Introduction

Malignancy, particularly hepatic carcinoma (HCC), has become one of the most life-threatening diseases in recent years. The chemotherapy, as one of cancer therapeutic methods, owns some side effects, despite of significant advances in this treatment (Carr, Vissers, & Cook, 2014). Therefore, treatments targeting of apoptosis in cancer are potential alternatives, which has been paid more and more attention (Kim & Kim, 2013). Polysaccharides, as one of natural compounds, have been used to enhance therapeutic efficacy through apoptosis induction of cancer cells without killing normal cells (Xu, Wu, Xu, Sun, Chen, & Yao, 2009).

Apoptosis is considered as a regulated active process signified by specific biochemical and morphological, during which individual cells undergo systematic self-destruction in response to various stimuli (Teodoro & Branton, 1997). There may be several multiple mechanisms for drug-induced apoptosis, and one of the most pivotal pathways in cells is the mitochondrial pathway (Tatsuta, Sugawara, Takahashi, Ogawa, Hosono, & Nitta, 2014), which is also important for polysaccharides inducing apoptosis in cancer cells (Hirahara, Edamatsu, Fujieda, Fujioka, Wada, & Tajima, 2013). A potential antitumor polysaccharide (LSPc1) has been purified from the fruiting bodies of *Lepista sordida* and proved to induce cancer apoptosis through the mitochondrial pathway (Miao, Mao, Pei, Miao, Xiang, Lv, et al., 2013). Atractylodes macrocephala polysaccharides (AMPs) have also been proved to induce apoptosis in glioma C6 cells via the mitochondrial pathway (Nasrallah & Horvath, 2014).

Polysaccharides could be obtained from various organisms, such as algae, plants, microorganisms and animals (Mehvar, 2003). Several reports have confirmed that polysaccharides, especially those extracted from fungi, exhibited various biological activities (Ali, Ziada, &

Blunden, 2009; Jeong, Jeong, Yang, Islam, Koyyalamudi, Pang, et al., 2010; Yu, LiHua, Qian, & Yan, 2009). It is noted that the activity of proliferation suppression and apoptosis of tumor cells has been extensively studied (Jeong, Koyyalamudi, Jeong, Song, & Pang, 2012; Zhang, Qi, Cheng, Liu, Huang, Wang, et al., 2014).

This work focuses on the apoptotic effects of PNA-2 (see **Supplementary data**) on HepG2 cells. And PNA-2 was proved to inhibit cell proliferation, induce cell-cycle arrest, activate the mitochondria-dependent apoptotic pathway, and block the migration as well as invasion of HepG2 cells. Furthermore, inhibition of Bcl-2, activation of cytochrome c and decrease of mitochondrial membrane potential induced by PNA-2 contributed to the apoptotic-inducing effect of HepG2 cells. Apoptotic pathway may play an important role in the inhibition of the tumor growth *in vivo*. Taken together, our findings indicate that PNA-2 triggers apoptosis in HepG2 cells through the mitochondria-dependent apoptotic pathway, dramatically inhibited the tumor growth, and may become a potential antitumor compound for liver cancer therapy.

2. Methods

2.1 Materials and reagents

PNA-2 was obtained as described in **Supplementary data**. Dulbecco's modified Eagle's medium (DMEM) with high glucose was purchased from Hyclone (Beijing, China). Fetal bovine serum (FBS) was obtained from Gibco GRL (Grand Island, NY, USA). Penicillin-streptomycin solution, trypsin, phosphate buffered saline (PBS, pH = 7.3), dimethyl sulfoside side (DMSO), 3-(4,5-dimethylthiazol-2-yl)-2,5-diphenyltertrazolium bromide (MTT), low-melting point agarose, normal-melting point agarose, and cell lysis solution were purchased from Solarbio (Beijing,

China). Propidium iodide (PI), Rhodamine 123, AO/EB were purchased from Sigma-Aldrich (St. Louis, MO, USA). RNeasy Mini Kit was purchased from Qiagen (Hilden, Germany). The PrimeScript 1st Strand cDNA Synthesis Kit was obtained from Takara Bio (Dalian, China). SYBR Green PCR master mix was purchased from Invitrogen (Shanghai, China). Antibodies against Cyt C, Bcl-2, Bax, α-tubulin,VDAC1, β-actin and fluorescent secondary antibodies labeled with FITC were purchased from Abcam (Shanghai, China). Polyvinylidene fluoride (PVDF) was purchased from Millipore (Shanghai, China). All chemicals and other reagents were of analytical grade.

2.2 Cells and Animals

HepG2 cells，human hepatic cancer cell line，were obtained from the Bioresource Collection and Research Center of the Food Industry Research and Development Institute (Hsinchu, Taiwan, ROC).

BALB/cAnN-nu mice at 4 to 6 weeks (female, 18−22 g) were provided by Beijing Vital River Biotechnology Company (SPF Certificate: No. SCXK (jing) 2013−0012, Beijing, China). The animals were kept according to the Guide for the Care and Use of Laboratory Animals (NRC 2011), and all experimental protocols were in accordance with Tianjin University of Science and Technology Medical College Animal Care Review Committee guidelines. The orthotopic inoculation protocol was approved by the Committee on the Use of Live Animals in Teaching and Research.

2.3 Cell culture

HepG2 cells were cultured in DMEM supplemented with 10% (v/v) fetal bovine serum and 1× penicillin/streptomycin (100 U/mL P and 0.1 mg/mL S), in a humidified atmosphere of 5% CO_2/95% air at 37 ^oC . After the cells were grown to 90% confluence in T25 tissue culture flasks

(TPP Biochrom AG, Trasadingen, Switzerland), they were plated at a desirable density for further assay. The plate was incubated at 37 ^{o}C overnight to allow cell attachment to the bottom. After the cell supernatant was removed, an aliquot with equal volume of test sample was added to the well.

2.4 Assessment of cell viability

The cell viability of HepG2 treated with PNA-2 at different concentrations (0, 6.25, 12.5, 62.5, 125, 250 and 500 μg/mL) was measured by MTT assay according to Lee *et al* (Lee, Yoon, & Park, 2008) with some modifications. HepG2 cells (8×10^4 cells/mL, 100 μL/well) treated with and without PNA-2 were cultured in 96-well plates for 48h. Then 20 μL of 5 mg/mL MTT dissolved in PBS was added to each well and incubated for another 4h. After the culture medium was discarded, 150 μL of DMSO was added to each well and the plate was oscillated for 15 min to dissovle the formazan completely. The absorbance was read at 570 nm with an ELISA reader (ASYS Hitech, GmbH, Austria), and the viability was calculated as follows:

$$Inhibition(\%) = \frac{A - B}{A - C} \times 100\%$$

where A is the average OD value of wells with untreated cells; B is the one of wells with PNA-2 treated cells; C is the one of without cells.

2.5 Invasiveness assay

The cells were seeded at a density of 1×10^5 cells per well in 24-well plates, and allowed to attach overnight. Then the supernatant was removed carefully and the wells was given a sharp smack with a 10 μl pipette tip gently and vertically. And plates were washed three times with PBS to remove the floating cells. Cells were treated by PNA-2 with concertrations of 0, , 12.5, 62.5 and 125 μg/mL for 24h and then examined under phase-contrast microscope (Olympus, Japan).

2.6 Observation of morphology changes

HepG2 cells (1×10^5 cells/mL) was inoculated on a cover slip, treated with PNA-2 (0, , 12.5, 62.5 and 125 μg/mL) for 24 h, and then pre-fixed with 2.5% glutaraldehyde at 4 ^{o}C for 30 min. In order to remove water thoroughly, the cells were then rinsed with PBS and ethanol in a gradient concentrations of 30%, 50%, 70%, 80%, 90%, 100%, respectively, with each rinse for 5 min. Finally, the surface morphology of cells treated with and without PNA-2 was characterized by SEM (Hitachi, Tokyo, Japan).

2.7 Acridine orange /ethidium bromide (AO/EB) staining

HepG2 cells treated with PNA-2 (0, 12.5, 62.5 and 125 μg/mL) were cultured in 24-well plates for 48h at 37 ^{o}C in an atmosphere of 5% CO_2. After washed three times with PBS and mixed with 4% paraformaldehyde for 10 min at 4 ^{o}C, cells were stained with AO/EB solution (100 μg/mL AO and 100 μg/mL EB in PBS) for 30 min at room temperature in the dark. Finally, cells was washed with PBS and observed by an inverted fluorescence microscope (AMG, USA).

2.8 Single cell gel electrophoresis assay

The HepG2 cells treated by PNA-2 and those without treated were plated at a density of 1×10^5 cells per dish and cultured for 48 h. Then operate was carried by comet assay according to Tice *et al* (Tice, Agurell, Anderson, Burlinson, Hartmann, Kobayashi, et al., 2000). Finally, comets were stained with ethidium bromide(5μg/ml) and analyzed by confocal laser scanning microscopy (Nikon, Tokyo, Japan).

2.9 Flow cytometric analysis

HepG2 cells (1×10^5 cells/mL) were seeded in T25 tissue culture flasks and exposed to various concentrations of PNA-2 (0, 12.5, 62.5 and 125μg/mL). The cells were washed with PBS, collected after trypsinization, and then fixed in 70% glacial ethanol. After washed with PBS for

three times, cells were resuspended in 1 mL of PBS containing 50 U/mL RNase and 50 μg/mL propidium iodide (PI), and then incubated for 40 min in the dark at 4 °C. Cell cycle analysis was performed by flow cytometry (BD, Franklin Lakes, NJ, USA) at an excitation wavelength of 488 nm, and the population of cells in each phase was calculated using the Modifit LT software program. Each experiment was carried out three times.

2.10 Rhodamine-123 staining

Changes in mitochondrial membrane potential (ΔΨm) due to mitochondrial dysfunction were detected using rhodamine-123 staining (J. Lemasters & Nieminen, 1997). The HepG2 cells in 24-well plates treated by PNA-2 with concentrations of 0, 12.5, 62.5 and 125μg/mL were cultured for 48h at 37 °C and 5% CO_2. After washed three times with PBS and fixed with 4% paraformaldehyde for 10 min at 4 °C, cells were stained with rhodamine-123 (5μg/mL) for 30min at room temperature in the dark. Finally cells were washed with PBS and observed by an inverted fluorescence microscope (AMG, USA).

2.11 Measurement of activities of caspase-9 and caspase-3

The assay was carried out to determine the proteolytic activity of Caspaes-3 and Caspaes-9. The HepG2 cells treated by different concentrations of PNA-2 (12.5, 62.5 and 125μg/mL) were separately collected. Then the activity of caspase-9 as well as caspase-3 was measured by caspase-3, 9 activity kit systems according to manufacturer's instructions (Beyotime Institute of Biotechnology, Haimen, China). The absorbance was measured by an ELISA reader at 405 nm.

2.12 Quantitative Real-time PCR

The expression of Caspaes-3, Caspaes-9, Bcl-2, Cytochrome C (Cyt C), CD31 and Ki67 of HepG2 cells treated with PNA-2 was analyzed by qRT-PCR. Cells were washed with PBS and

lysed using the lysis buffer provided by the kit. Total RNA was extracted using the RNeasy Mini-Kit according to the manufacturer's protocol. First-strand cDNA was synthesized using the PrimeScript1st Strand cDNA Synthesis Kit, with the Oligo dT-Adaptor Primer. Gene expression was monitored by qRT-PCR, carried out using the SYBR Green PCR master mix (Invitrogen). Primers for Caspaes-3, Caspaes-9, Bcl-2 and Cyt C and actin were designed (**Table 1**). RT-qPCR was performed using the ABI step one plus system (applied biosystems) followed by melting curve analysis with the following cycling program: initial activation at 95 ^{o}C for 2 min, followed by 48 cycles of denaturation at 95 ^{o}C for 15s, annealing at 55 ^{o}C for 30 s, and extension at 72 ^{o}C for 15s.

2.13 Western blot analysis

Whole cell lysates were denatured by boiling in loading buffer (20 mM Tris-HCl, pH 6.8, 10% glycerol, 4% SDS, 100 mM DTT and 0.04% bromophenol blue) for 5 minutes. Each sample (40 μg protein) was loaded onto 12% SDS polyacrylamide gel followed by electroblotting onto PVDF membrane. After blocking of non-specific binding with 5% nonfat milk (prepared in PBS containing 0.1% Tween 20) for 1 h at 37 ^{o}C, the membrane was applied with antibodies against Cyt C, Bcl-2 and β-actin, respectively. And this was followed by incubation with FITC labeled anti-rabbit antibody. Then the protein was detected using Infrared Imaging System (Odyssey, USA). Densitometry was performed using the software Quantity One.

2.14 Antitumor Activity In vivo

Mouse model of HepG2 was established by inoculating cells (4×10^{7} cells/mL, 100 μL) into the right shoulder of each mouse. After 24 h, the mice were divided into four groups with eight in each group at random. The experimental groups received different dosages of PNA-2 with 12.5,

62.5 and 125 mg/kg body weight, respectively. While the control group was administered 0.9% saline solution. PNA-2 or saline solution was administered using intragastric perfusion once daily. The tumor volume was measured from day 15. On the 30th day, the mice were weighed and sacrificed by cervical dislocation. Meanwhile, the tumor was excised and weighed.

2.14 Statistical analysis

Each experiment was repeated at least three times. Numerical data are presented as mean ± SEM. The difference between means was analyzed using one-way ANOVA. All statistical analyses were performed using SPSS 17.0 software (Chicago, IL, USA). Differences were considered significant if $P < 0.05$.

3. Results

3.1 Cell viability and migration ability of HepG2 cells treated by PNA-2

The antitumor activity of PNA-2 was investigated by an *in vitro* anticancer assay. After HepG2 cells treated with PNA-2 (0, 6.25, 12.5, 62.5, 125, 250 and 500 μg/mL) for 48 h, the cell inhibitory rate against cancer cell proliferation was determined. As shown in **Fig. 1A**, PNA-2 exhibited significant cytotoxicity at concentrations of 12.5, 62.5 and 125 μg/mL, and the inhibition rate decreased with reducing or increasing concentrations of PNA-2 at 6.25, 250 and 500 μg/mL. Therefore, cells were treated by various concentrations of PNA-2 with 12.5, 62.5 and 125 μg/mL for experiments hereafter.

Cell migration is an essential mechanism for various processes in unicellular and multicellular organisms, such as wound healing, immune responses and tissue formation (Glaß, Möller, Zirkel, Wächter, Hüttelmaier, & Posch, 2012), which is analyzed by cell scratch assay *in vitro* (Debeir, Adanja, Kiss, & Decaestecker, 2008; Liang, Park, & Guan, 2007). For the present study, wound

closure was examined at 0, 12 and 24 h in the presence of different concentrations of PNA-2 (0, 12.5, 62.5 and 125 μg/mL). As shown in **Fig. 1B**, non-treated cells migrated into the scratched area and filled the gap at 24 h, whereas the migration of HepG2 cells treated by PNA-2 was inhibited, especially at concentrations of 62.5 and 125 μg/mL for 24 h. The migration rates of HepG2 cells treated by PNA-2 of 12.5, 62.5, and 125 μg/mL for 12 h were 39.1%, 38.6%, and 41.3%, respectively, while those for 24 h were 60.4%, 58.3%, and 57.8% (**Fig. 1C**). Additionally, these datas exhibit significant difference from the control group ($P < 0.01$). All results suggested that the migration ability of HepG2 cells was inhibited by PNA-2 in a dose- and time-dependent manner.

3.2 Morphological change of HepG2 cells treated by PNA-2

Morphological changes of HepG2 cells treated with and without PNA-2 were characterized by SEM. **Fig. 2** showed that the microvilli on the surface of untreated cells remained intact, whereas typical apoptosis occurred to PNA-2-treated cells for phenomenons such as cell shrinkage, membrane blebbing, cytoplasmic vacuolization and so on. Thus PNA-2 indeed induces apoptosis in HepG2 cells .

3.3 Chromosome condensation and DNA damage of HepG2 Cells induced by PNA-2

Apoptotic, necrotic and viable HepG2 cells were scored under fluorescence microscope. A typical image of untreated cells with a green intact nuclear structure was observed in **Fig. 3A**. At 48-h treatment with PNA-2 at low doses of 12.5 and 62.5 μg/mL, cell apoptosis occurred (**Fig. 3B** and **C**) with marked nuclear condensation, membrane blebbing, nuclear shrinkage, as well as color changing from green to reddish-orange due to the binding of AO to denatured DNA, which indicated the programmed cell death of HepG2 cells induced by PNA-2 (illustrated by arrows). In

addition, necrosis was observed with the presence of red color at a high dose of 125 μg/mL (**Fig. 3D**). The ratios between red and green fluorescence of treated HepG2 cells indicated clearly that PNA-2 had a dose-dependent apoptogenic effect (**Fig. 3I**).

Furthermore, DNA damage was evaluated by Comet assay (or single-cell gel electrophoresis), a sensitivity method for detecting DNA strand breaks in individual cells. Cells treated by PNA-2 of 12.5 μg/ml showed some DNA damage with few comet tails, and comet tail length was significantly extended in those treated by PNA-2 of 62.5 and 125 μg/ml ($P < 0.05$ and $P < 0.01$, respectively) (**Fig. 3E-H**).

3.4 G0/G1 arrest in HepG2 cells induced by PNA-2

To explore the intrinsic mechanism by which PNA-2 inhibits cell proliferation, flow cytometry was performed on HepG2 cells with or without treatment with PNA-2 for 24 h (**Fig. 4A**). Compared with untreated cells, the significantly increased percentages of cells in G0/G1 phase (from 46.36% ± 4.03% to 67.66% ± 3.28%, $P < 0.01$), along with dramatically decreased cell population of S phase (from 34.04% ± 0.29% to 25.94% ± 0.24%, $P < 0.01$) as well as that of G2/M phase (from 18.91% ± 4.13% to 9.81% ± 0.6%, $P < 0.01$), were observed in HepG2 cells treated by PNA-2 of 125 μg/mL (**Fig.4B**). These data suggested that PNA-2 could inhibit the cell proliferation by inducing the G0/G1 arrest in a dose-dependent manner in HepG2 cells.

3.5 Mitochondria-dependent apoptosis triggered by PNA-2

Here, rhodamine-123, a membrane potential-specific dye, was used as a probe to monitor effects of PNA-2 on the mitochondrial function of HepG2 cell. As shown in **Fig. 5A**, green fluorescence significantly reduced in cells exposed to PNA-2 compared with that untreated by PNA-2. Treated by PNA-2 with concentrations of 12.5, 62.5, and 125 μg/ml, the mean

fluorescence intensity of cells represented significant loss ($P < 0.05$, $P < 0.01$, $P < 0.01$, respectively) (**Fig. 5B**), indicating that PNA-2-induced apoptosis was accompanied by mitochondrial membrane depolarization.

Furthermore, the potential mitochondria-dependent signaling molecules involved in PNA-2-mediated HepG2 cell proapoptosis, such as Cyt C and BCL-2, were investigated. Cyt C mRNA expression was significantly increased in a concentration-dependent manner, while that of BCL-2 protein was strongly inhibited by PNA-2 (**Fig. 5C**). Moreover, a 2.3-fold increase (0.89/0.39 = 2.3, **Fig. 5D**) and a reduction by 60% (1- 0.35/0.86 = 60%, **Fig. 5D**) in Cyt C and BCL-2 transcript levels were observed in cells treated at the highest concentration (125 μg/mL) (**Fig. 5E**). All results indicated that the mitochondria-dependent apoptotic pathway participated in PNA-2-induced HepG2 cell death.

3.6 Caspase-dependent apoptosis Induced by PNA-2

In order to determine whether a caspase-9-dependent pathway involved in the apoptosis induced by PNA-2, both caspase-3 and caspase-9 were analyzed, for caspase-3, as an apoptosis executioner, is responsible for degradation of cellular proteins and activated by caspase-9. **Fig. 6A** showed that the activities of caspase-9 and caspase-3 in HepG2 cells with treatment by PNA-2 (concentrations of 62.5 and 125μg/mL) for 48 h were significantly increased. Additionally, the gene expression profiles were further confirmed by quantitative fluorescence polymerase chain reaction, and **Fig. 6B** showed that exposure to various concentrations of PNA-2 resulted in changes in expressions of mitochondrial caspase-9 and caspase-3, which means that activation of caspase-9 and caspase-3 indeed participated in PNA-2-induced apoptosis in HepG2 cells.

3.7 Growth inhibition of transplantable tumors by PNA-2

Fed by PNA-2 with various concentrations of 12.5, 62.5 and 125 mg/kg, the tumor volume (**Fig. 7A**) and tumor weight (**Fig. 7 C**) gradually decreased in tumor-bearing mice. **Fig. 7B** indicated that PNA-2 could inhibit the tumor growth *in vivo* more intuitively. Moreover, mRNA expression of the angiogenetic factor CD31 as well as the proliferation marker Ki67 were significantly reduced in PNA-2 treated-tumors (**Fig. 7D**).

3.8 Release of Cytochrome c and Apoptosis-associated protein expression increased by PNA-2

One key characteristic in the intrinsic apoptotic pathway is the liberation of mitochondrial intermembrane proteins into the cytosol, such as cytochrome c, which plays a pivotal role in the activation of the caspase cascade. As shown in **Fig. 8A and B**, the level of cytosolic cytochrome c protein was dose-dependently upregulated over the test dosage rage of PNA-2. While PNA-2 caused a decrease in protein level of cytochrome c in the mitochondrial fraction at 62.5 and 125 mg/kg. Thus the results indicated that PNA-2 led to the release of cytochrome c from the mitochondria to the cytosol. For the Bcl-2 family members are important regulators of the mitochondrial apoptotic pathway, this study examined the expression of Bax and Bcl-2 proteins, in order to clarify the mechanism of PNA-2-induced apoptosis. **Fig. 8 C and D** revealed that protein levels of Bax increased dramatically in PNA-2-treated tumor-bearing groups at does of 62.5 and 125 mg/kg, whereas the protein expression level of Bcl-2 was decreased in a dose-dependent manner.

4. Discussion

Cancers are chronic diseases affecting millions of humans. It has been reported that medicinal mushrooms could serve as supplementary cancer treatments or direct remedies against cancer development (Jiang, Thyagarajan-Sahu, Loganathan, Eliaz, Terry, Sandusky, et al., 2012), for more and more medicinally compounds were evaluated (CFR Ferreira, A Vaz, Vasconcelos, &

306 Martins, 2010; Lull, Wichers, & Savelkoul, 2005). β-Glucans, derived from mushrooms, have
307 been focused on and recognized as a potential anticancer agent (Beaglehole & Horton, 2010;
308 Kodama, Harada, & Nanba, 2002).

309 PNA-2, a novel fungal polysaccharide purified from *P. nebrodensis* in our previous work,
310 contains β-(1,4)-linked-D-glucose main chains highly substituted with mannose units and
311 β-(1,3)-linked-D-glucose branches. Although some β-glucans, such as lentinan, schizophyllan,
312 maitake D-fraction, and *Ganoderma* polysaccharides, have been tested for potential antitumor
313 effects (Kodama, Murata, Asakawa, Inui, Hayashi, Sakai, et al., 2005; J. Li, Lei, Yu, Zhu, Zhang,
314 & Wu, 2007; Sreenivasulu, Vijayalakshmi, & Sambasivarao, 2010; Zhong, Liu, Tong, Zhong,
315 Wang, & Zhou, 2013), the antitumor activity of β-glucans branched of *P. nebrodensis* has not been
316 evaluated, and the mechanism is unclear, either.

317 In this study, PNA-2 anti-proliferative activities and inhibition of tumor metastasis on HepG2
318 cells were investigated. Results demonstrated significant inhibition on HepG2 cells with inhibition
319 rate of 34.2% at 125μg/mL and an rapid decrease of rates of migration from 88.2% to 57.8% at
320 24h (**Fig. 1**).

321 Apoptosis and cell cycle arrest are two main mechanisms for the cell growth inhibition (Sun et
322 al., 2011). Apoptosis is a process of cell suicide characterized by specific morphological changes
323 (Hagedorn & Sherwood, 2011), such as condensation of chromatin, loss of microvilli, blebbing
324 formation, and appearance of apoptotic bodies, which were observed in HepG2 cells treated by
325 PNA-2. Meanwhile, the important hallmarks of apoptosis, including the increase of AO/EB
326 staining apoptotic cells (**Fig. 2**) and evident DNA fragmentations (**Fig. 3**) was also displayed.
327 Moreover, cell cycle arrest is one of the key mechanisms by which anticancer drugs effect on the

cancer cells. Analysis of cell cycle was carried out to cells treated by PNA-2, and results indicated that the cell number in G0/G1 phases increased ($P < 0.01$), and that in S as well as G2/M phase decreased significantly ($P < 0.01$) (**Fig. 4**).

As reported, mitochondria plays a central role in initiating the apoptotic process and the loss of mitochondrial membrane potential ($\Delta\Psi m$) is as an early event in apoptosis (J. J. Lemasters, Holmuhamedov, Czerny, Zhong, & Maldonado, 2012; P. F. Li, Dietz, & von Harsdorf, 1999). Mitochondria of cancer cells have a higher membrane potential, poor permeability and less susceptible to activation of the mitochondrial pathway of apoptosis. Thus, to break the respiratory chain and damage mitochondrial membrane potential could become a fundamental indicator for the elimination of cancer cells (Gogvadze, 2011). Results in our work indicated that PNA-2 significantly depolarized the membrane potential in a dose-dependent manner (**Fig. 5A** and **B**). As known, the process of apoptosis is triggered by mitochondrial disruption and the subsequent release of Cyt C, with the expression changes of pro-apoptotic Bcl-2 family proteins and antiapoptotic proteins. And apoptosis is ultimately executed by the caspase family proteins. Here, we have found that levels of the cytosolic Cyt C are significantly increased in cells with PNA-2 treatment. which subsequently activates caspase 9. Activated caspase 9 by Cyt C protein in turn activates caspase 3, and activated caspase 3 ultimately induces apoptosis with a decrease in Bcl-2 levels (**Fig. 5A, B** and **C**). These results indicate that PNA-2 induces mitochondria-dependent apoptosis in HepG2 cells.

To further elucidate the role of PNA-2 *in vivo*, an HepG2 tumor model in BALB/cAnN-nu mice was established. Significant tumor suppressions of PNA-2 at concentrations of 12.5, 62.5, and 125 mg/kg were observed, and the mRNA expression of tumor cell proliferative markers such

as CD31 and Ki67 was also significantly decreased (**Fig. 7**). The mitochondria-mediated apoptotic pathway was under the control of multiple layers of regulation, and one of the most important players are members of Bcl-2 family. Results indicated that PNA-2 inhibited the expression of antiapoptotic protein Bcl-2, and also triggered the expression of proapoptotic protein Bax in HepG-2-bearing mice, which are necessary for the disruption of mitochondria and release of cytochrome c from mitochondria into cytosol (**Fig. 8**), and the activation of the mitochondria-dependent apoptotic signaling pathway.

Our data confirmed the potential of PNA-2 as an agent of cytostatic activity in HepG2 cells *in vitro* and *in vivo*, which may be valuable for application in drug developments. For further confirmation, other molecular mechanisms should be investigated to elucidate several molecular pathways and provide additional information on the potential use of this natural product in clinical settings.

5. Conclusion

In this study, the effect of PNA-2, a polysaccharide isolated from *P. nebrodensis* by alkaline extraction method in our previous work, on human hepatic cancer cells (HepG2) proliferation and apoptosis-related mechanism were investigated. The results suggested that PNA-2 could inhibit HepG2 cell proliferation, caused DNA damage and induced apoptosis via a mechanism primarily involving the activation of the intrinsic mitochondrial pathway.

Acknowledgments

We are grateful for the financial support provided by the Ph.D. Training Foundation of Tianjin University of Science and Technology (Grant No. 201402).

372

373 ## References

374 Ali, B. H., Ziada, A., & Blunden, G. (2009). Biological effects of gum arabic: a review of some recent
375 research. *Food and Chemical Toxicology, 47*(1), 1-8.
376 Beaglehole, R., & Horton, R. (2010). Chronic diseases: global action must match global evidence. *The*
377 *Lancet, 376*(9753), 1619-1621.
378 Carr, A. C., Vissers, M. C., & Cook, J. S. (2014). The effect of intravenous vitamin C on cancer-and
379 chemotherapy-related fatigue and quality of life. *Frontiers in oncology, 4*.
380 CFR Ferreira, I., A Vaz, J., Vasconcelos, M. H., & Martins, A. (2010). Compounds from wild
381 mushrooms with antitumor potential. *Anti-Cancer Agents in Medicinal Chemistry (Formerly*
382 *Current Medicinal Chemistry-Anti-Cancer Agents), 10*(5), 424-436.
383 Debeir, O., Adanja, I., Kiss, R., & Decaestecker, C. (2008). Models of cancer cell migration and
384 cellular imaging and analysis. *The Motile Actin System in Health and Disease*, 123-156.
385 Glaß, M., Möller, B., Zirkel, A., Wächter, K., Hüttelmaier, S., & Posch, S. (2012). Cell migration
386 analysis: Segmenting scratch assay images with level sets and support vector machines.
387 *Pattern Recognition, 45*(9), 3154-3165.
388 Gogvadze, V. (2011). Targeting mitochondria in fighting cancer. *Current pharmaceutical design,*
389 *17*(36), 4034-4046.
390 Hagedorn, E. J., & Sherwood, D. R. (2011). Cell invasion through basement membrane: the anchor cell
391 breaches the barrier. *Current opinion in cell biology, 23*(5), 589-596.
392 Hirahara, N., Edamatsu, T., Fujieda, A., Fujioka, M., Wada, T., & Tajima, Y. (2013). Protein-bound
393 polysaccharide-K induces apoptosis via mitochondria and p38 mitogen-activated protein
394 kinase‐dependent pathways in HL-60 promyelomonocytic leukemia cells. *Oncology reports,*
395 *30*(1), 99-104.
396 Jeong, S. C., Jeong, Y. T., Yang, B. K., Islam, R., Koyyalamudi, S. R., Pang, G., Cho, K. Y., & Song, C.
397 H. (2010). White button mushroom *Agaricus bisporus* lowers blood glucose and cholesterol
398 levels in diabetic and hypercholesterolemic rats. *Nutrition Research, 30*(1), 49-56.
399 Jeong, S. C., Koyyalamudi, S. R., Jeong, Y. T., Song, C. H., & Pang, G. (2012). Macrophage
400 immunomodulating and antitumor activities of polysaccharides isolated from Agaricus
401 bisporus white button mushrooms. *Journal of medicinal food, 15*(1), 58-65.
402 Jiang, J., Thyagarajan-Sahu, A., Loganathan, J., Eliaz, I., Terry, C., Sandusky, G. E., & Sliva, D. (2012).
403 BreastDefend™ prevents breast-to-lung cancer metastases in an orthotopic animal model of
404 triple-negative human breast cancer. *Oncology reports, 28*(4), 1139-1145.
405 Kim, M. H., & Kim, H. (2013). Oncogenes and tumor suppressors regulate glutamine metabolism in
406 cancer cells. *Journal of cancer prevention, 18*(3), 221.
407 Kodama, N., Harada, N., & Nanba, H. (2002). A polysaccharide, extract from Grifola frondosa, induces
408 Th-1 dominant responses in carcinoma-bearing BALB/c mice. *The Japanese Journal of*
409 *Pharmacology, 90*(4), 357-360.
410 Kodama, N., Murata, Y., Asakawa, A., Inui, A., Hayashi, M., Sakai, N., & Nanba, H. (2005). Maitake
411 D-Fraction enhances antitumor effects and reduces immunosuppression by mitomycin-C in
412 tumor-bearing mice. *Nutrition, 21*(5), 624-629.
413 Lee, S.-M., Yoon, M.-Y., & Park, H.-R. (2008). Protective effects of Paeonia lactiflora pall on hydrogen

peroxide-induced apoptosis in PC12 cells. *Bioscience, biotechnology, and biochemistry, 72*(5), 1272-1277.

Lemasters, J., & Nieminen, A. (1997). Mitochondrial oxygen radical formation during reductive and oxidative stress to intact hepatocytes. *Bioscience reports, 17*, 281-291.

Lemasters, J. J., Holmuhamedov, E. L., Czerny, C., Zhong, Z., & Maldonado, E. N. (2012). Regulation of mitochondrial function by voltage dependent anion channels in ethanol metabolism and the Warburg effect. *Biochimica et Biophysica Acta (BBA)-Biomembranes, 1818*(6), 1536-1544.

Li, J., Lei, L., Yu, C., Zhu, Z., Zhang, Q., & Wu, S. (2007). [Effect of Ganoderma lucidum polysaccharides on tumor cell nucleotide content and cell cycle in S180 ascitic tumor-bearing mice]. *Nan fang yi ke da xue xue bao= Journal of Southern Medical University, 27*(7), 1003-1005.

Li, P. F., Dietz, R., & von Harsdorf, R. (1999). p53 regulates mitochondrial membrane potential through reactive oxygen species and induces cytochrome c-independent apoptosis blocked by Bcl-2. *The EMBO Journal, 18*(21), 6027-6036.

Liang, C.-C., Park, A. Y., & Guan, J.-L. (2007). In vitro scratch assay: a convenient and inexpensive method for analysis of cell migration in vitro. *Nature protocols, 2*(2), 329-333.

Lull, C., Wichers, H. J., & Savelkoul, H. F. (2005). Antiinflammatory and immunomodulating properties of fungal metabolites. *Mediators of inflammation, 2005*(2), 63-80.

Mehvar, R. (2003). Recent trends in the use of polysaccharides for improved delivery of therapeutic agents: pharmacokinetic and pharmacodynamic perspectives. *Current pharmaceutical biotechnology, 4*(5), 283-302.

Miao, S., Mao, X., Pei, R., Miao, S., Xiang, C., Lv, Y., Yang, X., Sun, J., Jia, S., & Liu, Y. (2013). *Lepista sordida* polysaccharide induces apoptosis of Hep-2 cancer cells via mitochondrial pathway. *International journal of biological macromolecules, 61*, 97-101.

Nasrallah, C. M., & Horvath, T. L. (2014). Mitochondrial dynamics in the central regulation of metabolism. *Nature Reviews Endocrinology, 10*(11), 650-658.

Sreenivasulu, K., Vijayalakshmi, M., & Sambasivarao, K. R. (2010). Regulation studies of telomerase gene in cancer cells by lentinan. *Avicenna journal of medical biotechnology, 2*(4), 181.

Tatsuta, T., Sugawara, S., Takahashi, K., Ogawa, Y., Hosono, M., & Nitta, K. (2014). Cancer-Selective Induction of Apoptosis by Leczyme. *Molecular and Cellular Oncology, 4*, 139.

Teodoro, J. G., & Branton, P. E. (1997). Regulation of apoptosis by viral gene products. *Journal of virology, 71*(3), 1739.

Tice, R., Agurell, E., Anderson, D., Burlinson, B., Hartmann, A., Kobayashi, H., Miyamae, Y., Rojas, E., Ryu, J., & Sasaki, Y. (2000). Single cell gel/comet assay: guidelines for in vitro and in vivo genetic toxicology testing. *Environmental and molecular mutagenesis, 35*(3), 206-221.

Xu, H.-S., Wu, Y.-W., Xu, S.-F., Sun, H.-X., Chen, F.-Y., & Yao, L. (2009). Antitumor and immunomodulatory activity of polysaccharides from the roots of *Actinidia eriantha*. *Journal of ethnopharmacology, 125*(2), 310-317.

Yu, Z., LiHua, Y., Qian, Y., & Yan, L. (2009). Effect of *Lentinus edodes* polysaccharide on oxidative stress, immunity activity and oral ulceration of rats stimulated by phenol. *Carbohydrate Polymers, 75*(1), 115-118.

Zhang, X.-r., Qi, C.-h., Cheng, J.-p., Liu, G., Huang, L.-j., Wang, Z.-f., Zhou, W.-x., & Zhang, Y.-x. (2014). *Lycium barbarum* polysaccharide LBPF4-OL may be a new Toll-like receptor 4/MD2-MAPK signaling pathway activator and inducer. *International immunopharmacology,*

458 *19*(1), 132-141.
459 Zhong, K., Liu, L., Tong, L., Zhong, X., Wang, Q., & Zhou, S. (2013). Rheological properties and
460 antitumor activity of schizophyllan produced with solid-state fermentation. *International*
461 *journal of biological macromolecules, 62*, 13-17.

462

Figures caption:

Fig.1.Cell viability and migration ability assay. A Inhibitory effects of PNA-2 on the cell viability of HepG2 cells by MTT. (n = 6), * P<0.05, **P<0.01 vs. control. **B.** Cell starch assay of PNA-2 on HepG2 cells at different dosage and times. **C.** The standerd of migration rate of PNA-2 on HepG2 cells.

Fig.2. The changes of cell surface observed by SEM. HepG2 cells were treated with PNA-2 of A. 0 μg/mL, B. 12.5 μg/mL, C. 62.5 μg/mL, D. 125 μg/mL.

Fig.3. PNA-2 induces apoptosis in HepG2 cells. A-D. Effect of PNA-2 with different concentrations of 0 μg/mL, 12.5 μg/mL, 62.5 μg/mL and 125 μg/mL on morphological changes in HepG2 cells stained by AO/EB. Apoptosis occurred when the cell nuclei were red or reddish-orange (scale bar: 200 μm). **E-H.** Comets were analyzed by confocal laser scanning microscopy at 543 nm (scale bar: 200 μm) **I.** The changes of % Red/Green-fluorescence of HepG2 cells treated by PNA-2. **J.** The length of comet tails increased in the presence of PNA-2.

Fig.4. PNA-2 induces cell cycle arrest in HepG-2 cells. A. Representative flow cytomeric analysis for DNA content in HepG2 cells treated by PNA-2 with different concentrations of 0 μg/mL, 12.5 μg/mL, 62.5 μg/mL and 125 μg/mL. Results were expressed as percentage of cells in G0/G1, S, and G2/M-phase. **B.** Graphical analysis of cell cycle phase distribution corresponding to A. (* P<0.01, **P<0.01 vs. control.).

Fig.5. PNA-2 triggers mitochondria- mediate pathway. A. Loss of the mitochondrial membrane potential (ΔΨm) (scale bar: 200 μm); **B.** The mean fluorescence intensity of 20 cells selected at random; **C.** Bcl-2 and Cyt C mRNA expression in HepG2 cells treated by PNA-2 with different concentrations of 0 μg/mL, 12.5 μg/mL, 62.5 μg/mL and 125 μg/mL; **D.** PNA-2-induced changes

in protein expressions of Cyt C and Bcl-2 in HepG2 cells determined by Western blot; **E.** The standard of fold expression of Cyt C and Bcl-2 in HepG2 cells (* P<0.01, **P<0.01 vs. control.)

Fig.6. PNA-2 induces apoptosis through caspase-dependent manner. A. Effects of PNA-2 at different concentrations of 0 μg/mL, 12.5 μg/mL, 62.5 μg/mL and 125 μg/mL on caspase-9 and caspase-3 activation (mean±SEM, n = 3) (* P<0.01, **P<0.01 vs. control.). **B.** mRNA expressions of Caspase-3 and Caspase-9 in HepG2 cells treated by PNA-2 at different concentrations of 0 μg/mL, 12.5 μg/mL, 62.5 μg/mL and 125 μg/mL.

Fig. 7. Antitumor effect of PNA-2 *in vivo*. **A**. The average tumor volume calculated at indicated time points in HepG2-bearing female nude mice (n = 8, per group). **B**. Tumors were isolated on day 30, tumors formed in each group were photographed and 3 representative tumors from 4 different mice were displayed. **C**. Tumor weights determined on day 30. **D**. CD31 and Ki67 mRNA expression of the tumor in HepG2-bearing mouse treated with PNA-2. Bars represent SEM. Significance was calculated with Student's t test.* P < 0.05 and **P < 0.01 vs control.

Fig. 8. Western blot analysis of Cyt C release and the expression of Bcl-2 family in tumor. **A**. The cytosolic and mitochondria proteins were analyzed by western blot with Cyt C. **B**. The standard of fold expression of Cyt C in HepG2 tumor cells. **C.** Total protein extracts were prepared and then analyzed by western blot with antibodies to Bcl-2, Bax and β-actin. **D.** Analysis of ratio of Bcl-2 and Bax. Bars represent SEM. Significance was calculated with Student's t test. (* P<0.01, **P<0.01 vs. control)

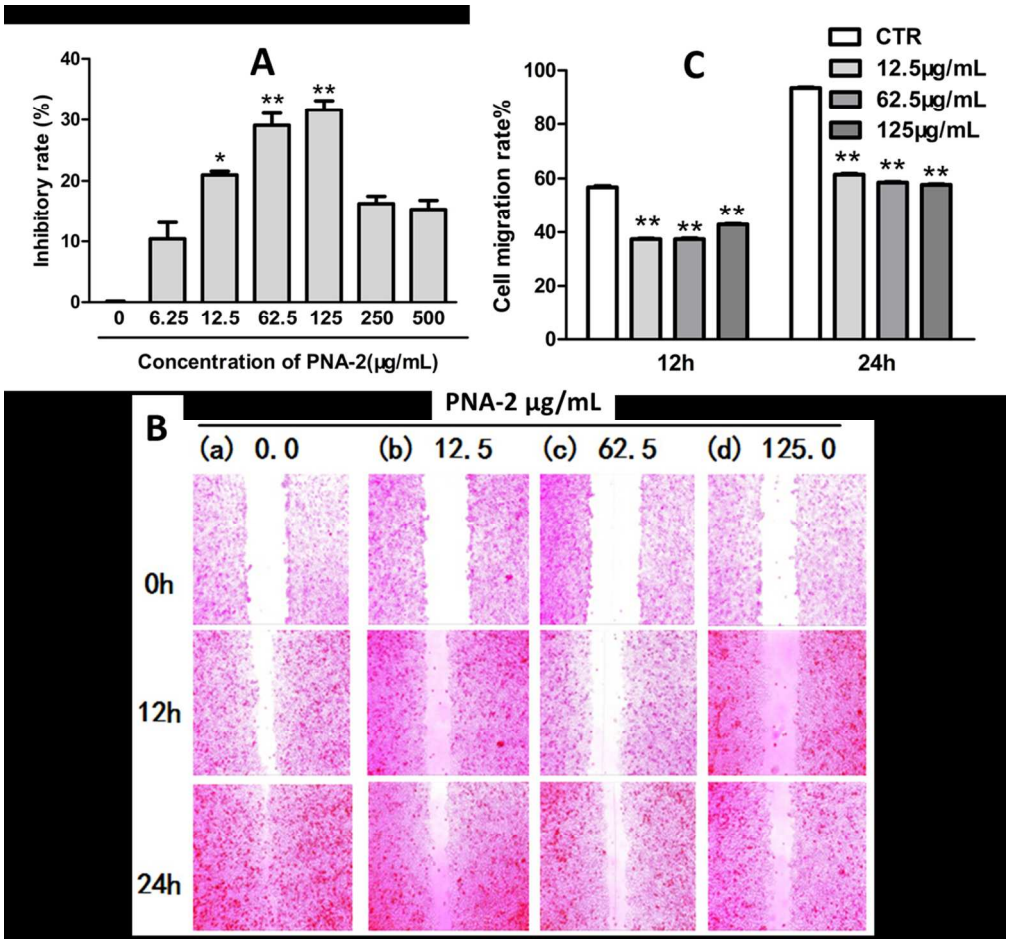

202x188mm (150 x 150 DPI)

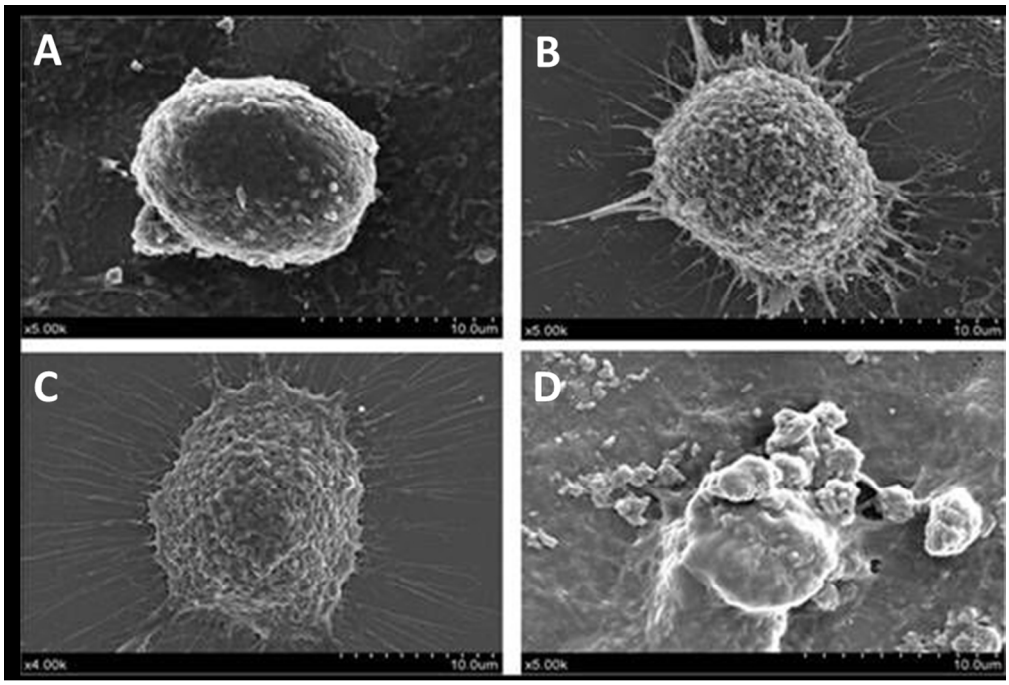

204x138mm (150 x 150 DPI)

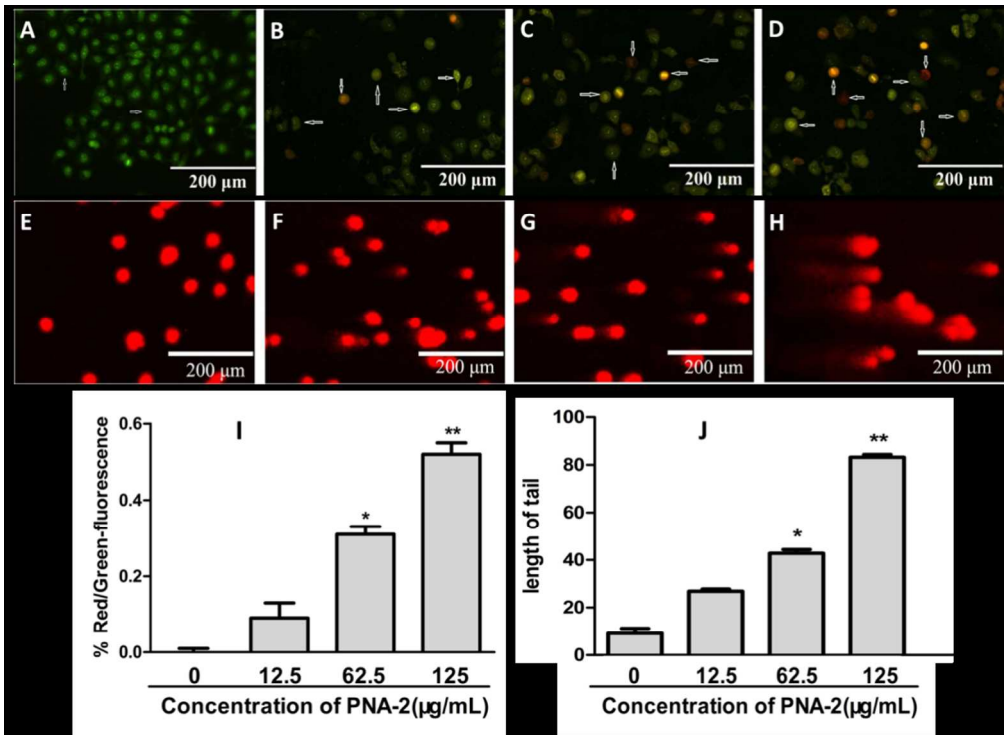

146x106mm (220 x 220 DPI)

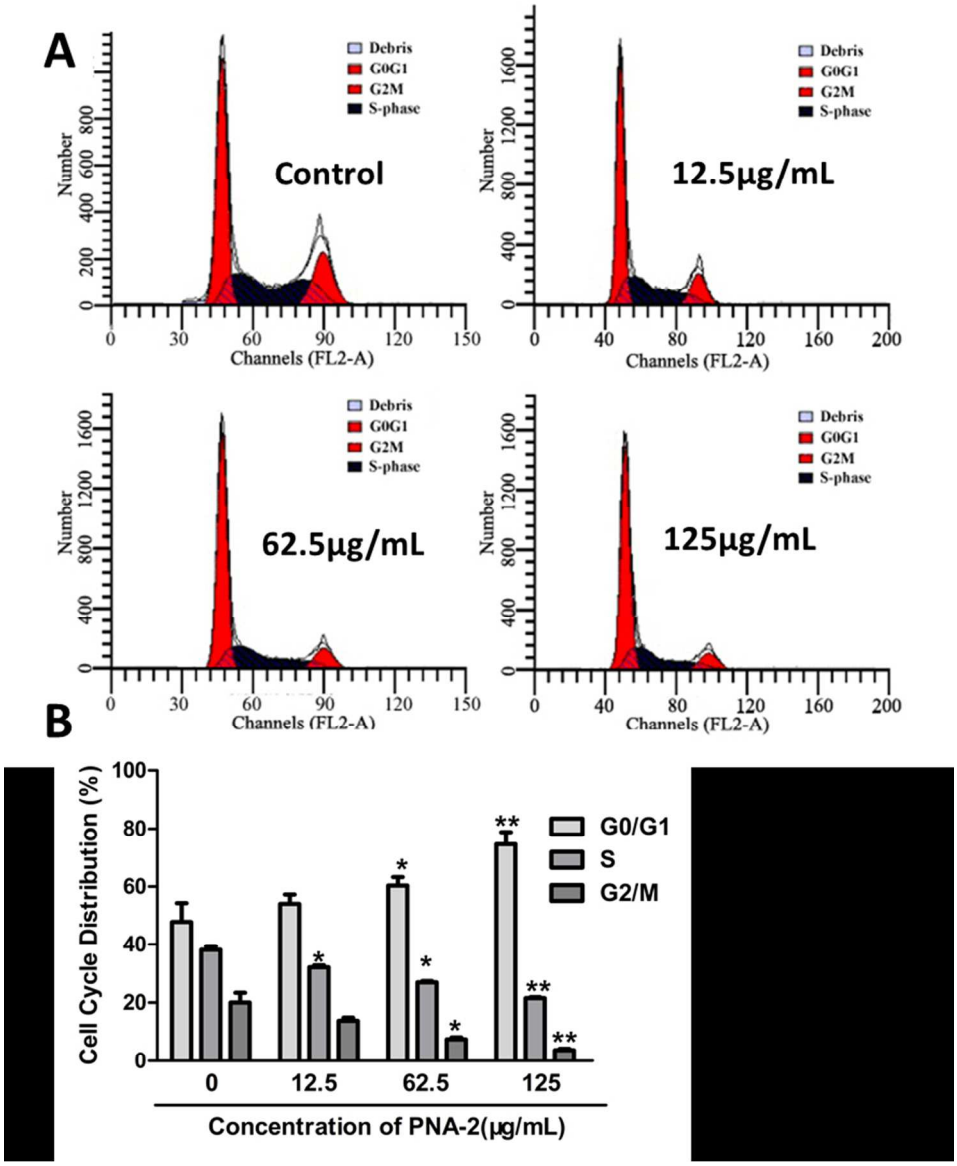

149x188mm (150 x 150 DPI)

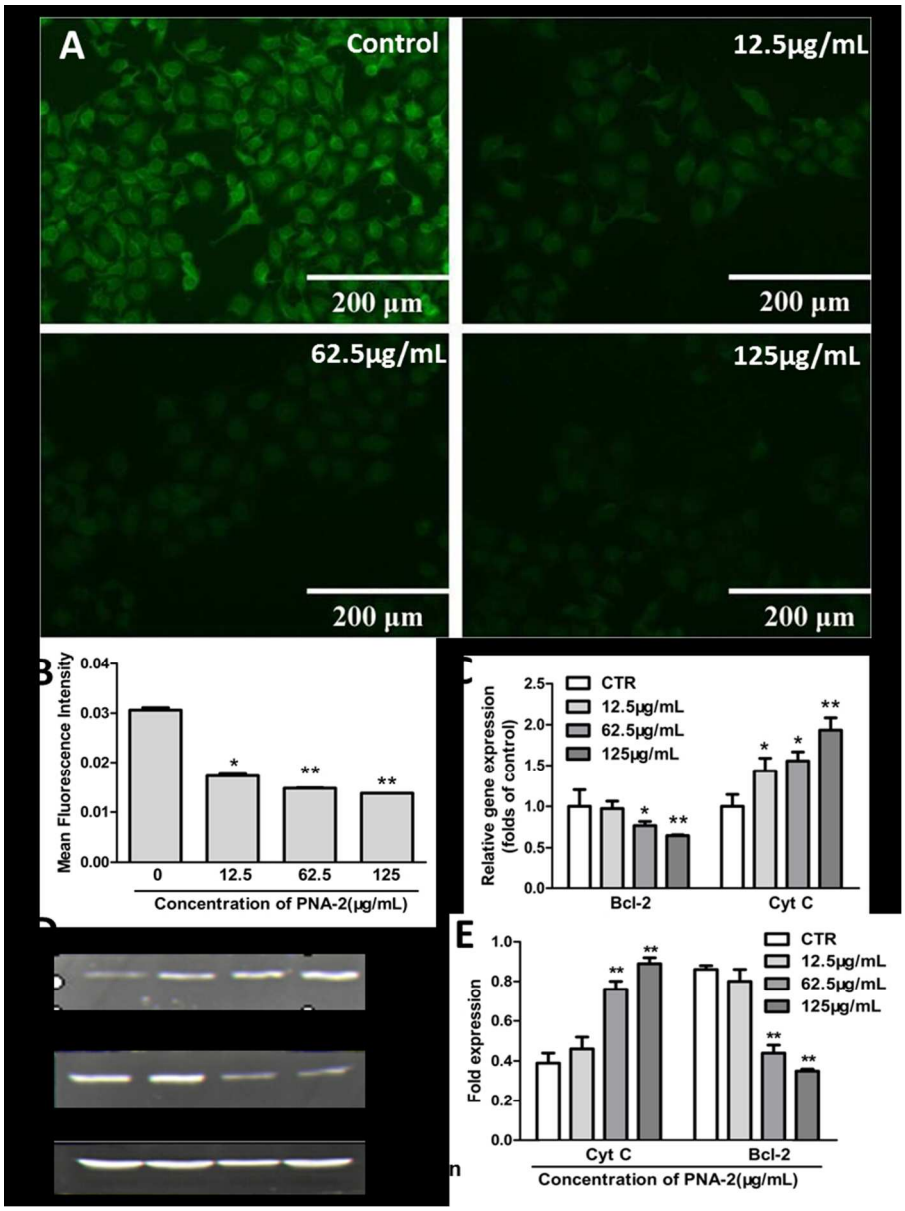

147x197mm (150 x 150 DPI)

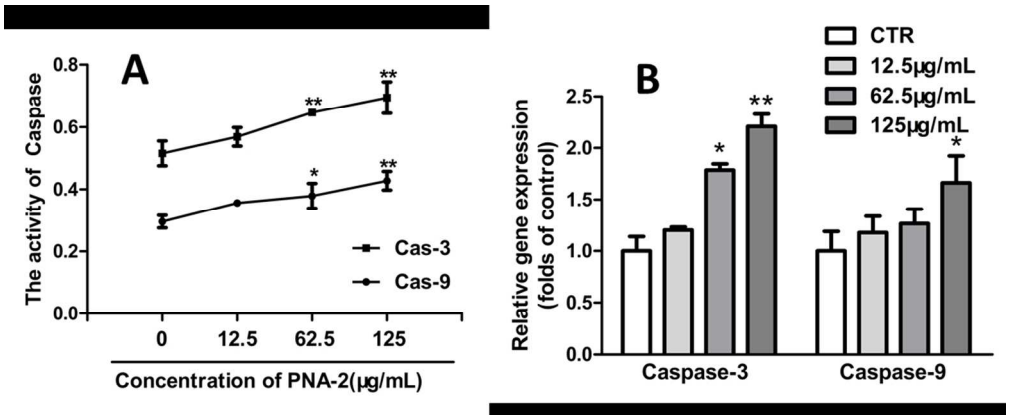

210x86mm (150 x 150 DPI)

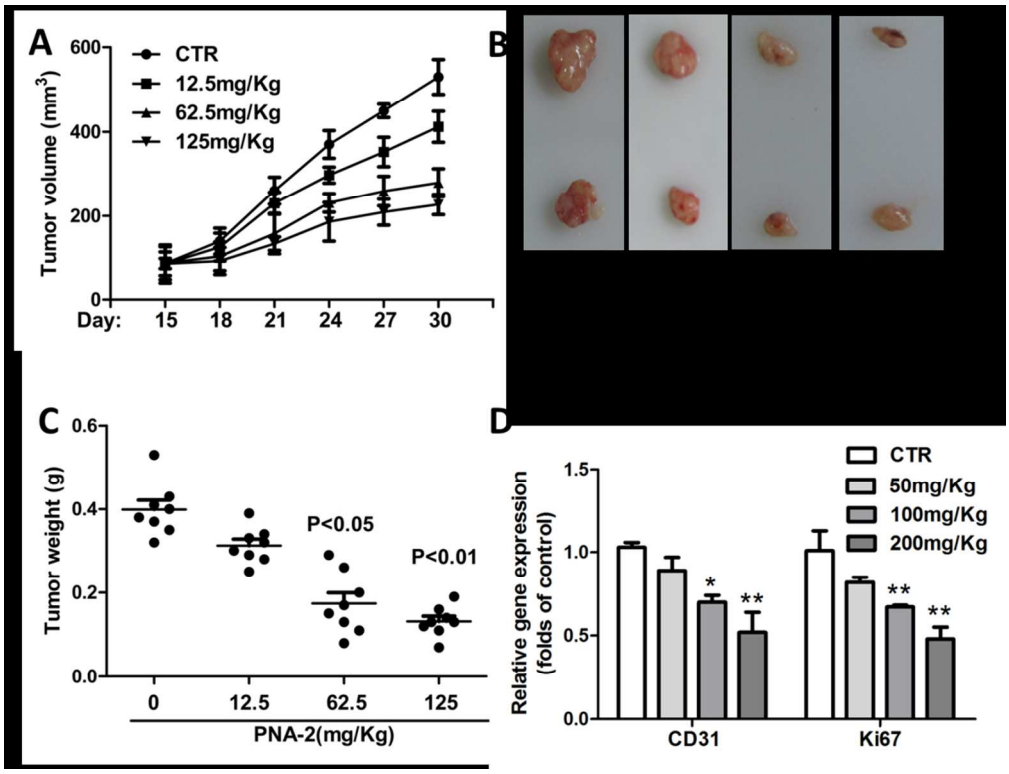

146x111mm (220 x 220 DPI)

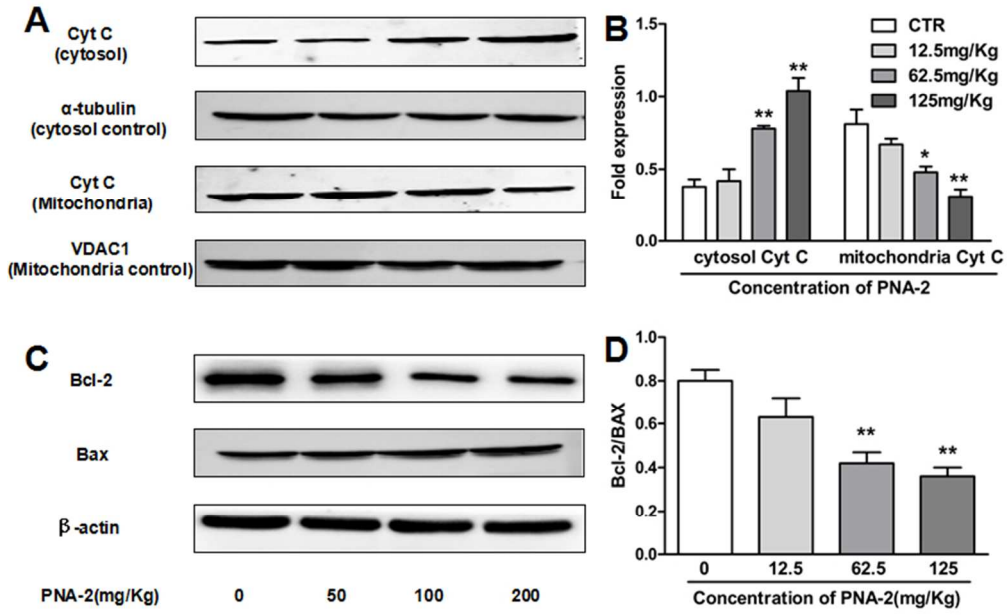

209x132mm (96 x 96 DPI)

Table 1. Sequences of gene-specific qRT-PCR primers

Gene	Sequence of primers(upstream / downstream)
Casp-3	TGTGAGGCGTTGTAGAAGTT / CGCTTCCATGTATGATCTTTGGT
Casp-9	TGGAGACTCGAGGGAGTCAG / TCGACAACTTTGCTGCTTGC
Bcl-2	GATAACGGAGGCTGGGATGC / TCACTTGTGGCCCAGATAGG
Cyt C	CGTTGAAAAGGGAGGCAAGC / TCTCCCCAGATGATGCCTTTG
Ki67	AACCTGCAAAGCGGAACGTG / CATTTGCCAGTTCCTCAGTGTG
CD31	GACGTGCAGTACACGGAAGT / TCTGCTTTCCACGGCATCAG
β-actin	AACTGGAACGGTGAAGGTGA / GTGCAATCAAAGTCCTCGGC

PNA-2 mediated mitochondria-dependent apoptosis in HepG2 cells in vitro and vivo.